Reversibility of bound-to-continuum transitions induced by a strong short laser pulse and the semiclassical uniform approximation

Einat Frishman and Moshe Shapiro
Department of Chemical Physics, The Weizmann Institute of Science, Rehovot 76100, Israel
(Received 11 March 1996)

We show that the problem of the net absorption of one photon from a strong laser pulse in a bound-to-continuum transition can be recast as a single integral equation. For a certain class of absorption spectra, this integral equation can be converted to a second-order Schrödinger-like differential equation, which can be accurately solved in an essentially closed form using the semiclassical uniform approximation. With the aid of the integral equation and the uniform solutions we find that for strong short pulses, irreversible transitions to a perfectly absorbing continuum in the weak-field regime become reversible. In particular, continuum levels may execute Rabi oscillations with the precursor bound state. These oscillations occur at different frequencies, depending on the continuum energy. As a result, spectral migrations and formations of transparent lines may occur. Field-induced interferences between neighboring lines is also investigated. [S1050-2947(96)10010-X]

PACS number(s): 32.80.Rm, 42.50.Vk

I. INTRODUCTION

Calculations of molecular photodissociation have been confined in the past to a large extent to the weak-field regime [1–9]. The methodology used in these calculations constitutes a hybrid of exact propagation methods to deal with the (strong) molecular interactions and perturbative approaches to deal with the (assumed weak) field-matter interactions. The situation has changed in the last few years with the desire of theorists to treat with greater precision molecular dissociation and (atomic) ionization processes induced by strong laser pulses. Thus, theories which treat the photodissociation of simple molecules [10–20] and ionization of atoms [21–27] in a nonperturbative way have been developed.

The excitation of continuum-state resonances has been discussed for a sharply turned-on constant amplitude field [6,10,28,29]. However, the cw field problem is different from the smooth pulse problem to be treated here. Not only the is mathematical treatment more complicated in the latter case, the physical outcome of smooth pulse excitation are quite different.

Most of the methods based on the above photodissociation and ionization theories are purely numerical. They essentially constitute the brute-force solution of the time-dependent or time-independent field-matter Schrödinger equation. As such, they do not make use of the availability of weak-field methods and the abundance of material matrix elements generated in weak-field calculations. Recently [30,31], we have shown that by invoking the ''flat'' or ''slowly varying'' continuum approximation (SVCA) we can utilize weak-field matrix elements to obtain the strong-field one-photon ionization or dissociation rates. Of particular importance is that the method is capable of yielding the product-state distribution of fragments resulting from the dissociation of molecules. In this way one can obtain the strong-field photodissociation yields at the cost of the weak-field calculations.

While it was anticipated that for intermediate-to-strong fields the SVCA method is quite accurate, its range of validity has not been established. In the present paper we examine this point by developing an exact theory of the one-photon dissociation and ionization problem. As in the SVCA, our theory builds on the same material matrix elements used in the weak-field theories while making no approximation beyond the rotating-wave approximation. This is done by recasting the problem as an integral equation in one temporal dimension, whose numerical solution can be attained with very modest computational efforts. We then show that for a certain class of absorption spectra, this integral equation can be converted to a second-order differential equation that is homomorphic to the one spatial-dimension time-independent Schrödinger equation. Using the arsenal of methods available for solving such equations, and in particular the uniform technique [32,33], this equation can be readily solved in an essentially analytic manner. With the aid of the integral equation and the uniform solutions we investigate the various factors affecting strong pulse-induced one-photon transitions to multiple continua.

II. THEORY OF PULSED ONE-PHOTON TRANSITIONS TO A CONTINUUM

We consider a molecule breaking apart, or being ionized as a result of the action of a laser pulse of electric field

$$\vec{\varepsilon}=\hat{\vec{\varepsilon}}\varepsilon'(t)\cos(\omega_L t). \tag{1}$$

The total Hamiltonian is

$$H_{\rm tot}=H_M-\vec{\mu}\cdot\vec{\varepsilon}(t), \tag{2}$$

where H_M is the radiation free material Hamiltonian and $\vec{\mu}$ is the transition dipole operator.

Assuming that the field is in near resonance with transitions from the initial bound state ψ_1 to the $\psi(E,\mathbf{n}^-)$ continuum of states, where both ψ_1 and $\psi(E,\mathbf{n}^-)$ are eigenstates of H_M,

$$[E_1-H_M]\psi_1=[E-H_M]\psi(E,\mathbf{n}^-)=0, \tag{3}$$

we expand the full time-dependent wave function as [2,34,35],

$$\Psi(t)=b_1(t)\psi_1\exp(-iE_1t/\hbar)+\sum_n\int dE\,b_{E,\mathbf{n}}(t)\psi(E,\mathbf{n}^-)\exp(-iEt/\hbar). \quad (4)$$

Insertion of Eq. (4) into the time-dependent Schrödinger equation,

$$i\hbar\,\partial\Psi/\partial t=H_{\rm tot}\Psi(t), \quad (5)$$

and use of the orthogonality of the eigenfunctions of H_M, results in a set of first-order integrodifferential equations for the b_1 and $b_{E,\mathbf{n}}$ coefficients,

$$i\hbar\,\frac{db_1}{dt}=-\int dE\sum_n\,\mu(1|E,\mathbf{n})\varepsilon(t)b_{E,\mathbf{n}}(t)\times\exp[-i(\omega_{E,1}-\omega_L)t], \quad (6)$$

$$b_{E,\mathbf{n}}(t)=\frac{-1}{i\hbar}\,\mu(E,\mathbf{n}|1)\int_{-\infty}^{t}dt'\varepsilon(t')b_1(t')\times\exp[i(\omega_{E,1}-\omega_L)t']. \quad (7)$$

In the above, $\mu(E,\mathbf{n}|1)\equiv\langle\psi(E,\mathbf{n}^-)|\mu|\psi_1\rangle$, $\omega_{E,1}\equiv(E-E_1)/\hbar$. Only the ''rotating wave'' terms have been retained.

We can solve the above set of integrodifferential equations by first substituting Eq. (7) in Eq. (6), resulting in an equation involving the $b_1(t)$ coefficient only,

$$\frac{db_1}{dt}=\frac{-1}{\hbar^2}\int dE\sum_n\,|\mu(E,\mathbf{n}|1)|^2\varepsilon(t)\int_{-\infty}^{t}dt'\varepsilon(t')\times\exp[-i(\omega_{E,1}-\omega_L)(t-t')]b_1(t'). \quad (8)$$

The integrodifferential equation in b_1 can be simplified by first calculating $F(t-t')$, the Fourier transform of the absorption spectrum

$$F(t-t')=\int dE A(E)\exp[-i\omega_{E,1}(t-t')], \quad (9)$$

where $A(E)$, the absorption spectrum, is given as

$$A(E)\equiv\sum_{\mathbf{n}}\,|\mu(E,\mathbf{n}|1)|^2. \quad (10)$$

Knowledge of $F(t-t')$, which may be termed the ''spectral autocorrelation function'' [30,31,35,36], allows us to rewrite Eq. (8) as

$$\frac{db_1}{dt}=\frac{-1}{\hbar^2}\,\varepsilon(t)\int_{-\infty}^{t}dt'\varepsilon(t')F(t-t')\times\exp[i\omega_L(t-t')]b_1(t'). \quad (11)$$

There are a number of spectral shapes for which $F(t-t')$ is separable. For example if the spectrum has a Lorentzian shape,

$$A(E)=\Gamma_s/[(E-\mathcal{E}_s)^2+\Gamma_s^2/4], \quad (12)$$

and using the fact that $t>t'$, we have that

$$\exp[i\omega_L(t-t')]F(t-t')=f_s^+(t)f_s^-(t'), \quad (13)$$

where

$$f_s^{\pm}(t)=\sqrt{2\pi}\exp[\mp i\chi_s t], \quad (14)$$

and $\chi_s\equiv\Delta_s-i(\Gamma_s/2\hbar)$, where $\Delta_s\equiv(\mathcal{E}_s-E_1)/\hbar-\omega_L$ is the detuning of the laser central frequency relative to $\mathcal{E}_s$.

Under these circumstances Eq. (11) transforms into two coupled first-order differential equations,

$$\frac{db_1}{dt}=\frac{i}{\hbar}\,\varepsilon(t)f_s^+(t)B_s(t),$$

$$\frac{dB_s}{dt}=\frac{i}{\hbar}\,\varepsilon(t)f_s^-(t)b_1(t), \quad (15)$$

which can be solved in a routine way [although care must be taken to renormalize the exponentially growing $f_s^-(t)$ function].

In general, $F(t-t')$ is not separable but it is possible to transform Eq. (8) to a discrete set of differential equations by some variant of the Laplace transform method. Our variant starts by expressing the dipole moment matrix elements $\mu(1|E,\mathbf{n})$ as a sum of (overlapping or isolated) resonances,

$$\mu(1|E,\mathbf{n})=\sum_{s=1}^{N}\,\frac{i\mu_{s\mathbf{n}}\Gamma_s/2}{E-\mathcal{E}_s+i\Gamma_s/2}, \quad (16)$$

where $\mu_{s\mathbf{n}}$ are derived by fitting Eq. (16) to a given spectrum. The spectrum now becomes

$$A(E)=\sum_n\,|\mu(1|E,\mathbf{n})|^2=\sum_{s's}\,\frac{\mu_{s's}^2\Gamma_s\Gamma_{s'}/4}{(E-\mathcal{E}_s+i\Gamma_s/2)(E-\mathcal{E}_{s'}-i\Gamma_{s'}/2)}, \quad (17)$$

where $\mu_{s's}^2\equiv\Sigma_n\mu_{s\mathbf{n}}\mu_{s'\mathbf{n}}^*$. If we only keep the diagonal ($s=s'$) terms $A(E)$ becomes a sum of Lorentzians. The off-diagonal terms allow for interferences between overlapping resonances; hence the form of Eq. (17) is quite general.

The Fourier transform of $A(E)$ [remembering that in Eq. (11) $t>t'$] now becomes

$$\exp[i\omega_L(t-t')]F(t-t')=2\pi\sum_s\,\alpha_s\exp[-i\chi_s(t-t')]=\sum_s\,\alpha_s f_s^+(t)f_s^-(t'), \quad (18)$$

where

$$\alpha_s\equiv\sum_{s'}\,\frac{-i\mu_{s's}^2\Gamma_s\Gamma_{s'}/4}{\mathcal{E}_s-\mathcal{E}_{s'}-i(\Gamma_s+\Gamma_{s'})/2}, \quad (19)$$

and $f_s^{\pm}$ are defined in Eq. (14).

With Eq. (18) we can transform Eq. (8) into a discrete set of coupled differential equations,

$$\frac{db_1}{dt}=\frac{i}{\hbar}\sum_s \alpha_s\varepsilon(t)f_s^+(t)B_s(t), \tag{20}$$

$$\frac{dB_s}{dt}=\frac{i}{\hbar}\,\varepsilon(t)f_s^-(t)b_1(t), \quad s=1,\ldots,N. \tag{21}$$

These equations can be solved in a routine way using a variety of propagation methods of first-order differential equations. Having obtained $b_1(t)$, the continuum coefficient $b_{E,\mathbf{n}}$ can be computed as a straightforward quadrature according to Eq. (7).

III. THE UNIFORM AND WKB APPROXIMATIONS

When the features in the continuum are not much sharper than the laser bandwidth, or the separation between the resonances is larger than the laser bandwidth, the above set of coupled equations [Eqs. (20) and (21)] can be reduced to a single second-order equation. By differentiating Eq. (20) we obtain that

$$\frac{d^2b_1(t)}{dt^2}=\frac{d\ \ln\varepsilon(t)}{dt}\frac{db_1(t)}{dt}-\frac{2\pi\varepsilon^2(t)}{\hbar^2}\sum_s \alpha_s b_1(t) - \frac{\varepsilon(t)}{\hbar}\sum_s \alpha_s\chi_s f_s^+(t)B_s(t), \tag{22}$$

where we have used the explicit form of f_s^+ [Eq. (14)]. We now define $\chi(t)$ as,

$$\sum_s \alpha_s\chi_s f_s^+(t)B_s(t)=\chi(t)\sum_s \alpha_s f_s^+B_s(t), \tag{23}$$

using which, we obtain from Eqs. (20) and (22), that

$$\frac{d^2b_1}{dt^2}=\left(\frac{d\ \ln\varepsilon(t)}{dt}-i\chi(t)\right)\frac{db_1}{dt}-\frac{2\pi}{\hbar^2}\,\varepsilon^2(t)\alpha b_1, \tag{24}$$

where $\alpha=\Sigma_s\alpha_s$.

This second-order differential equation in time is homomorphic to a one-dimensional time-independent Schrödinger equation in a spatial variable. This can be easily seen by denoting

$$g_1(t)=-\frac{d\ \ln\varepsilon(t)}{dt}+i\chi(t), \tag{25}$$

$$g_0(t)=\frac{2\pi}{\hbar^2}\,\varepsilon^2(t)\alpha, \tag{26}$$

writing Eq. (24) as

$$\frac{d^2b_1}{dt^2}+g_1(t)\,\frac{db_1}{dt}+g_0(t)b_1=0, \tag{27}$$

and transforming $b_1(t)$, according to

$$c(t)=\exp\left(\tfrac{1}{2}\int^t g_1(t')dt'\right)b_1(t) =\varepsilon(t)^{-1/2}\exp\left(\frac{i}{2}\int^t\chi(t')dt'\right)b_1(t). \tag{28}$$

We obtain a Schrödinger-like equation in $c(t)$,

$$\left(\frac{d^2}{dt^2}-W(t)\right)c(t)=0, \tag{29}$$

where

$$W(t)=\tfrac{1}{2}g_1'(t)+\tfrac{1}{4}g_1^2(t)-g_0(t) =-\frac{d\varepsilon(t)}{2dt}\frac{d^2\ln\varepsilon(t)}{dt^2}+\frac{1}{4}\left(\frac{d\ \ln\varepsilon(t)}{dt}-i\chi(t)\right)^2 -\frac{2\pi}{\hbar^2}\,\varepsilon^2(t)\alpha. \tag{30}$$

The ''time-dependent potential,'' $W(t)$, is analogous to minus the local momentum squared, $-p^2(x)$, of the time-independent Schrödinger equation. $W(t)$ can be complex, with the imaginary part depending on $\Delta(=\Sigma_s\alpha_s\Delta_s f_s^+B_s)$ the average detuning of the laser's center frequency ω_L with respect to the various resonances that contribute to continuum.

For a single resonance Eq. (23) is an identity, and we of course know what the (time-independent) χ function is. When there are more resonances, $\chi(t)$ cannot be determined without knowing $b_1(t)$, since by Eq. (21),

$$\chi(t)=\frac{\Sigma_s\alpha_s\chi_s f_s^+\int^t dt'\,\varepsilon(t')f_s^-(t')b_1(t')}{\Sigma_s\alpha_s f_s^+\int^t dt'\,\varepsilon(t')f_s^-(t')b_1(t')}. \tag{31}$$

In practical applications we find that we can approximate $\chi(t)$ as

$$\chi(t)\approx\chi^0(t)=\frac{\Sigma_s\alpha_s\chi_s f_s^+\int^t dt'\,\varepsilon(t')f_s^-(t')}{\Sigma_s\alpha_s f_s^+\int^t dt'\,\varepsilon(t')f_s^-(t')}. \tag{32}$$

Thus, for a Gaussian pulse envelope centered about t_0,

$$\varepsilon(t)=\varepsilon_L\exp\left[-\left(\frac{t-t_0}{2\delta}\right)^2\right], \tag{33}$$

we can calculate χ^0 via the identity [35],

$$\int^t dt'\,\varepsilon(t')f_s^-(t')=\pi\sqrt{2}\varepsilon_L\delta\,\exp(-\delta^2\chi_s^2) \times\{1+\mathrm{erf}(t/2\delta-i\,\delta\chi_s)\}. \tag{34}$$

The time-dependent potential assumes the form

$$W(t)=\frac{-(t-t_0)}{8\delta^4}\,\varepsilon_L\,\exp\left[-\left(\frac{t-t_0}{2\delta}\right)^2\right]-\frac{2\pi}{\hbar^2}\,\alpha\varepsilon_L \times\exp\left[-2\left(\frac{t-t_0}{2\delta}\right)^2\right]-\frac{1}{4}\left(\frac{t-t_0}{\delta^2}-i\chi^0(t)\right)^2. \tag{35}$$

In complete analogy to the case of the time-independent Schrödinger equation, we call time points satisfying the $W(t^*)=0$ equation, ''turning points.'' If there is only one turning point, the solutions of Schrödinger-like equation [Eq. (29)] can be written to an excellent approximation in terms of the uniform regular and irregular Airy functions Ai(T) and Bi(T) [37],

$$c_{\rm uni}(t)=\left(\frac{T(t)}{-W(t)}\right)^{1/4}\{C_a{\rm Ai}(-T(t))+C_b{\rm Bi}(-T(t))\}, \tag{36}$$

where the complex argument T is defined as

$$T(t)=\left(\frac{3}{2}\int_{t^*}^{t}\sqrt{-W(t')}dt'\right)^{2/3}, \tag{37}$$

and C_a and C_b are constants determined by the initial conditions, $b_s(-\infty)=1$ and $b_s'(-\infty)=0$. If there are no turning points on the real time-axis we choose the complex turning point which is closest to the relevant time range.

The uniform approximation is the exact solution of the equation

$$\left(\frac{d^2}{dt^2}-W(t)-\eta(t)\right)c_{\rm uni}(t)=0, \tag{38}$$

where

$$\eta(t)=[T'(t)]^{1/2}\frac{d^2}{dt^2}[T'(t)]^{-1/2}. \tag{39}$$

It is an excellent approximation to Eq. (29), because usually $|\eta(t)|\ll|W(t)|$. If there is more than one turning point, the Airy functions can still be used (provided the turning points do not coalesce), by by writing the solutions of Eq. (36) for each time-interval containing a turning point and matching these solutions and their derivatives across the time-intervals. Usually no more than two turning points exist.

It is also of interest to use a number of simpler approximations: The first constitutes the (zero-order) WKB approximation,

$$b_1(t)=\exp\left[-\tfrac{1}{2}\int^t g_1(t')dt'\right]\left\{C_a\exp\left[\int_{t^*}^{t}[W(t')]^{1/2}dt'\right]+C_b\exp\left[-\int_{t^*}^{t}[W(t')]^{1/2}dt'\right]\right\}, \tag{40}$$

and the second being slowly varying continuum approximation (SVCA) [30]. The SVCA can be invoked when Γ_s is large relative to the effective bandwidth of the laser pulse. For many direct dissociations the absorption spectrum extends over thousands of wave numbers [38] and it is justifiable to approximate $F(t-t')$ of Eq. (18) by letting $\Gamma_s\to\infty$. In order to increase all the Γ_s widths at a uniform rate we parametrize Γ_s as

$$\Gamma_s=\Gamma\gamma_s, \tag{41}$$

and let $\Gamma\to\infty$. We obtain that

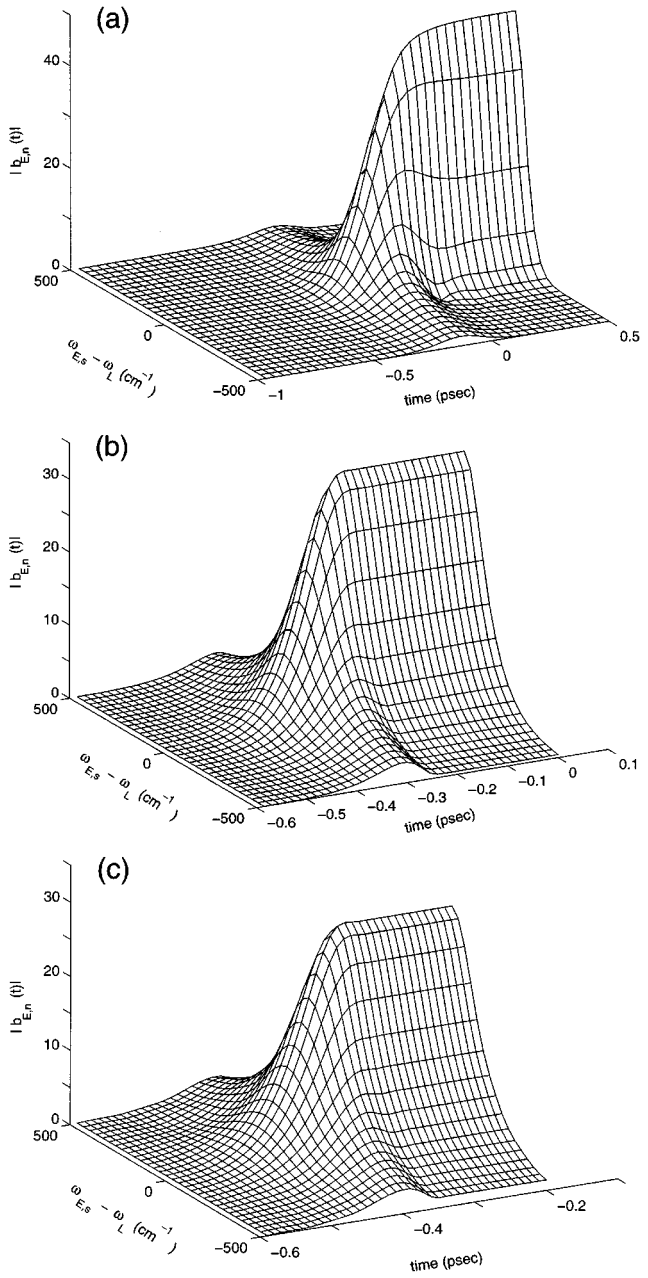

FIG. 1. Temporal evolution of the continuum coefficient $b_{E,\mathbf{n}}$ for different pulse intensities at the center of the absorption spectrum. The spectral width (Γ_s) is fixed at 2000 cm^{-1}, the laser bandwidth is fixed at 120 cm^{-1}, and the dipole strength (α_s) is fixed at 2.8×10^{-3}. (a) Peak-height=0.01 a.u., (b) peak height=0.1 a.u., (c) peak height=0.5 a.u.

$$F(t-t')=2\pi\sum_s\alpha_s\exp[(-i\mathcal{E}_s-\Gamma_s/2)(t-t')/\hbar]$$

$$\overset{\Gamma\to\infty}{\to}2\pi\hbar\overline{\mu^2}\delta(t-t'), \tag{42}$$

where, using Eqs. (41) and (19),

$$\overline{\mu^2}=\sum_{s's}\frac{2\mu_{s's}^2\gamma_{s'}}{\gamma_s+\gamma_{s'}}. \tag{43}$$

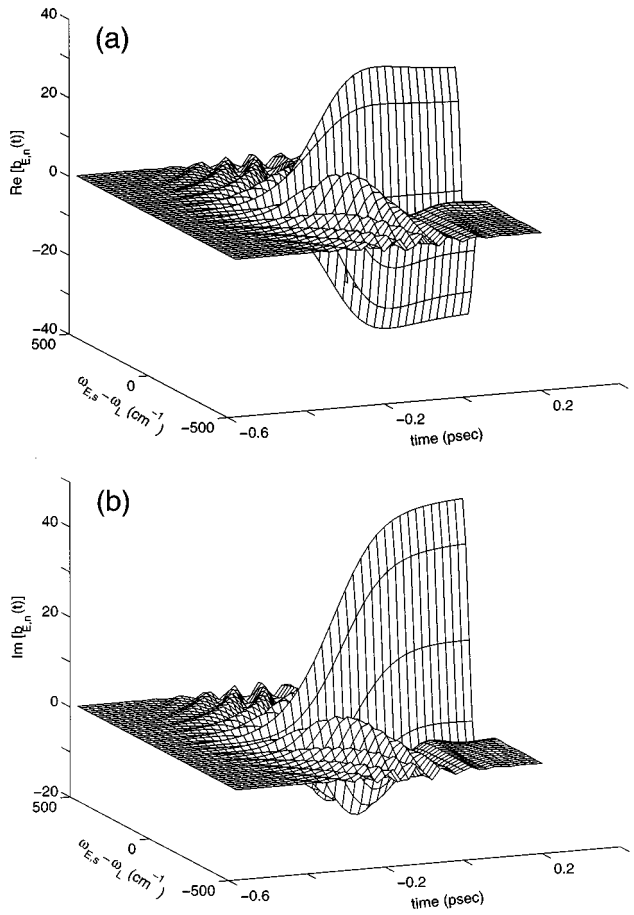

FIG. 2. (a) Real and (b) imaginary parts of the $b_{E,\mathbf{n}}$ continuum coefficients. The spectral and pulse parameters are as in Fig. 1(c).

The SVCA approximation of Eq. (42) greatly simplifies Eq. (11), which now becomes

$$\frac{db_1}{dt} = -\frac{\pi}{\hbar}\,\overline{\mu^2}\varepsilon^2(t)b_1(t), \tag{44}$$

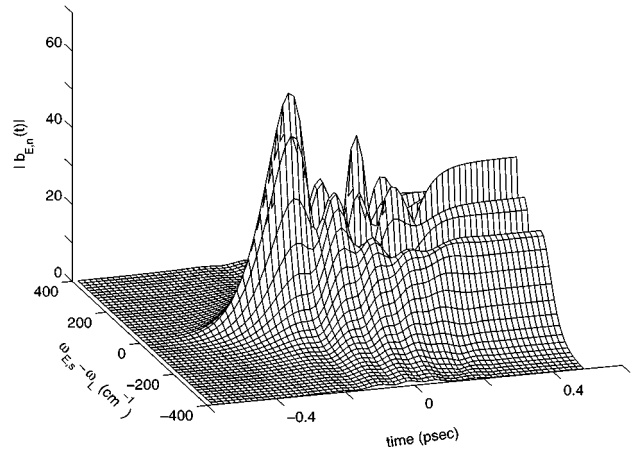

FIG. 3. Temporal evolution of the continuum coefficients at the center of the absorption spectrum for a narrow absorption band, $\Gamma_s = 50\ \mathrm{cm}^{-1}$. Other parameters are pulse's bandwidth$=120\ \mathrm{cm}^{-1}$, pulse's peak height$=0.05$ a.u., transition dipole strength $(\alpha_s) = 5.7\times10^{-5}$.

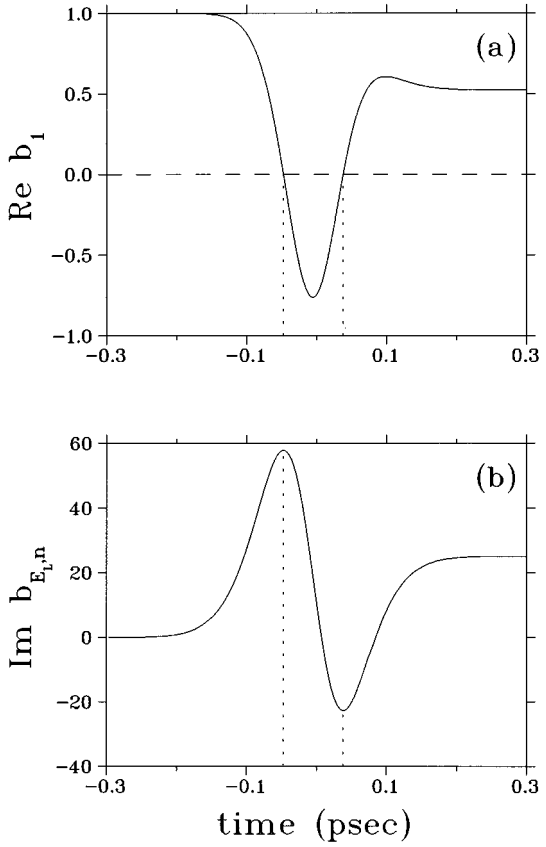

FIG. 4. Bound-state coefficient (b_1) and center-line continuum coefficient $(b_{E,\mathbf{n}})$ for a pulse whose bandwidth is 250 cm^{-1}. Other parameters are as in Fig. 3. The laser center frequency is in resonance with the spectral line center, hence, b_1 is real and $b_{E,\mathbf{n}}$ is imaginary.

i.e.,

$$b_1(t) = b_1(-\infty)\exp\left(-\frac{\pi}{\hbar}\,\overline{\mu^2}\int_{-\infty}^{t}\varepsilon^2(t')dt'\right). \tag{45}$$

A ''slowly varying'' continuum acts as a perfect absorber, since in this approximation $b_1(t)$ decreases monotonically with time. When the structures in the continuum are narrower than the effective bandwidth of the pulse (which depends on its frequency profile *and* its intensity), we expect the SVCA approximation to break down and Rabi oscillations to emerge.

IV. COMPUTATIONS

A. Transition probabilities to a continuum

We first present studies of the effect of the pulse intensity on the transition probabilities to a slowly varying continuum. We consider a continuum composed of single broad Lorentzian of width $\Gamma_s = 2000\ \mathrm{cm}^{-1}$, excited by a 120-$\mathrm{cm}^{-1}$-wide pulse (i.e., a pulse of $\sim$80 fsec duration). The center frequency of the pulse is tuned to the center of the continuum $(\Delta_s = 0)$.

In Figs. 1(a)–1(c) we present the $|b_{E,\mathbf{n}}(t)|$ continuum coefficients as a function of time, at different intensities. The

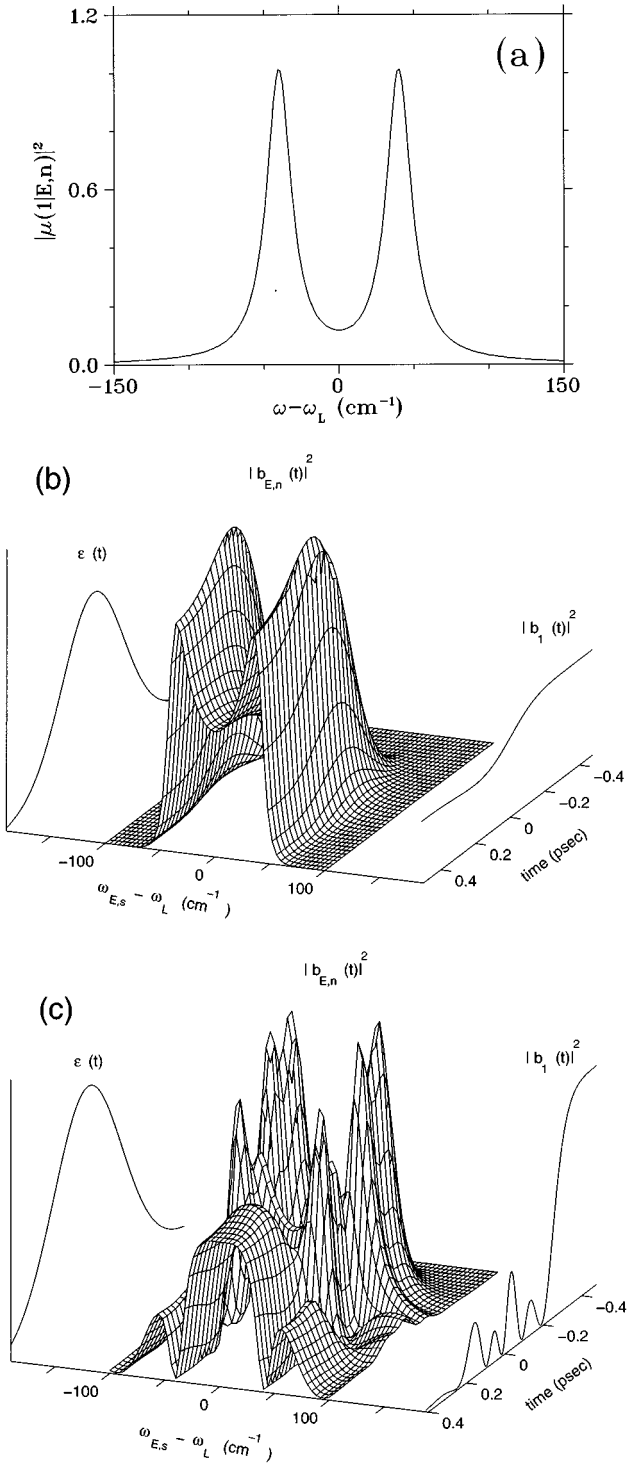

FIG. 5. Temporal evolution of the continuum populations for a bound-free spectrum comprised of two Lorentzians, with $\mu_{1,\mathbf{n}}=\mu_{2,\mathbf{n}}=1$, $\Gamma_1=\Gamma_2=20$ cm^{-1}, $\Delta_1=-40$ cm^{-1}, $\Delta_2=40$ cm^{-1}. The pulse bandwidth is 100 cm^{-1}. (a) The weak-field absorption spectrum; (b) $|b_{E,\mathbf{n}}|^2$ as a function of t and E, for $\varepsilon_L=5\times10^{-3}$ a.u.; (c) The same as in (b), for $\varepsilon_L=5\times10^{-2}$ a.u.

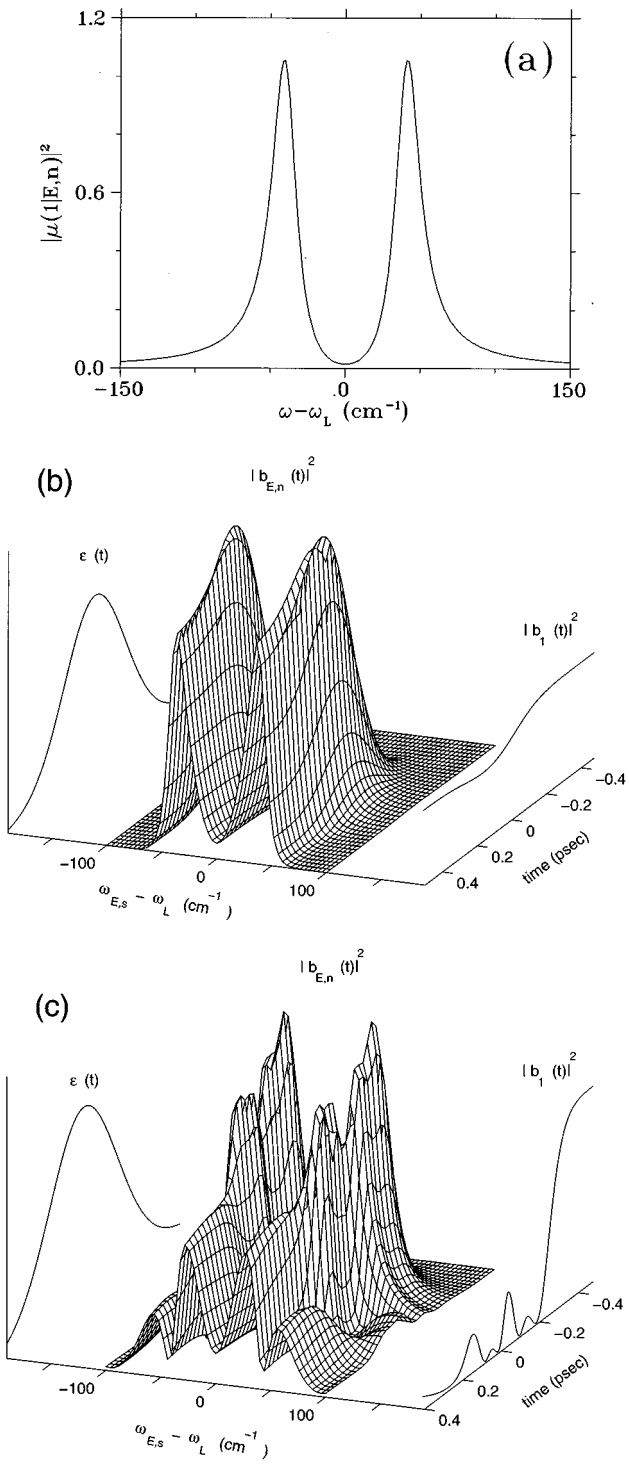

FIG. 6. Temporal evolution of the continuum populations for a bound-free spectrum comprised of two overlapping resonances. (a) The weak-field absorption spectrum; (b) $|b_{E,\mathbf{n}}|^2$ as a function of t and E, for $\varepsilon_L=5\times10^{-3}$ a.u.; (c) The same as in (b), for $\varepsilon_L=5\times10^{-2}$ a.u.

onset of off-resonance processes is typified by a nonmonotonic behavior: At off-pulse-center energies, the continuum coefficients rise and fall with the pulse, with the effect becoming more pronounced the further away from the line center the continuum energy levels are. In the far wings of the pulse the continuum coefficients are zero at the end of the pulse, giving rise to a pure transient, otherwise known as a ''virtual'' state.

As we increase the field strength, the continuum line shapes [given as $|b_{E,\mathbf{n}}(t=\infty)|$] broaden. This broadening is due to saturation of the continuum population, which is greater for continuum states near the pulse center than at the

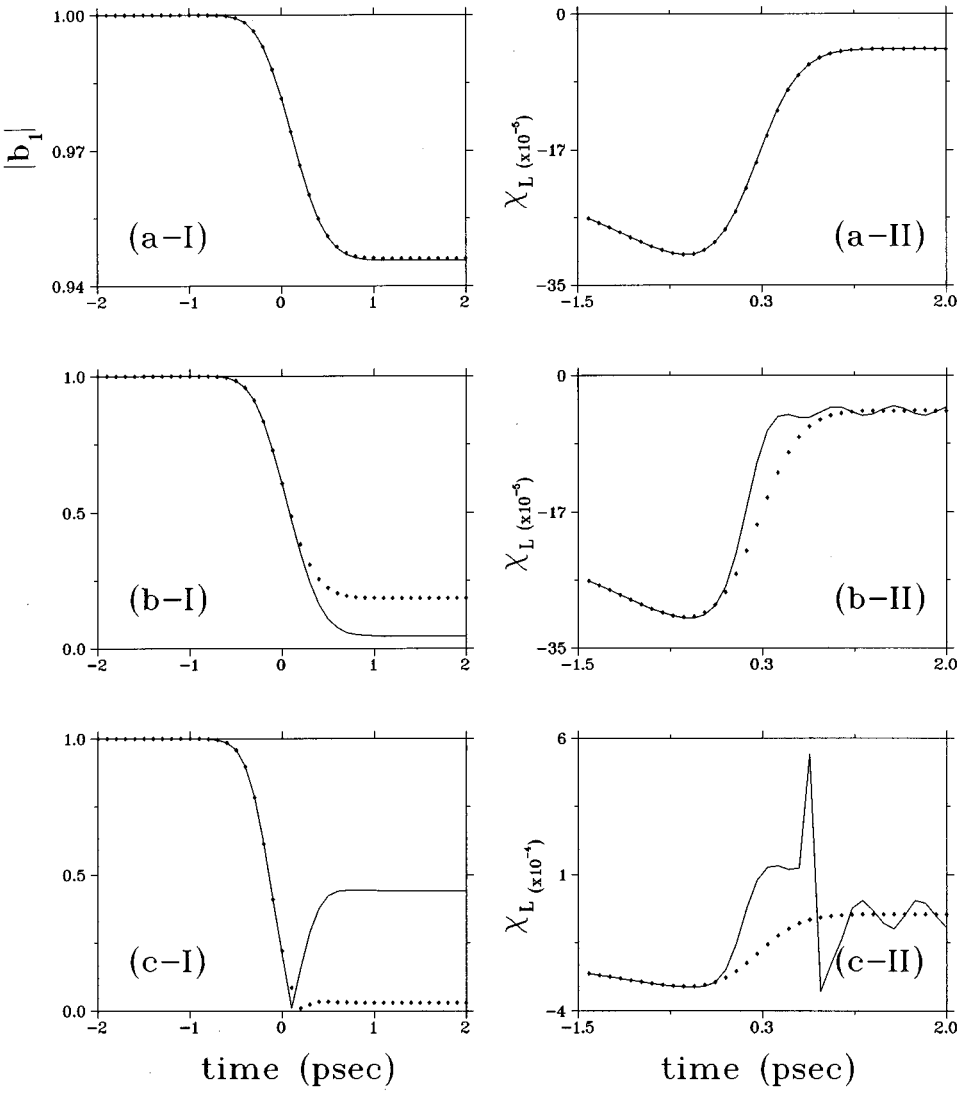

FIG. 7. Comparison of $b_1(t)$, the bound-state coefficient, obtained numerically and by the single Schrödinger-like equation for different pulse amplitudes. Exact results, full line; single Schrödinger-like equation results, dotted line. The pulse bandwidth is 50 cm^{-1}. The spectrum is composed of three resonances with, $\mu_{1\mathbf{n}}=\mu_{2\mathbf{n}}=\mu_{3\mathbf{n}}=1$, $\Gamma_1=\Gamma_2=\Gamma_3=20$ cm^{-1}, $\Delta_1=0$ cm^{-1}, $\Delta_2=-60$ cm^{-1}, $\Delta_3=60$ cm^{-1} (a) $\varepsilon_L=1\times10^{-3}$ a.u. (b) $\varepsilon_L=5\times10^{-3}$ a.u. (c) $\varepsilon_L=8\times10^{-3}$ a.u.

pulse wings. For example, for the relatively weak pulse of peak height of 0.01 a.u., shown in Fig. 1(a) the continuum linewidth is $\sim$100 cm^{-1}, i.e., roughly that of the pulse itself. As we increase the pulse field to the peak value of 0.1 a.u., the continuum lines broaden beyond the pulse linewidth, assuming the width of $\sim$200 cm^{-1}. At peak-heights of 0.5 a.u. the continuum linewidth is already $\sim$300 cm^{-1}.

The slowly varying continuum is almost a perfect absorber. Therefore, as we increase the pulse intensity we empty the initial state (ψ_1) faster and the dissociation or ionization is over before any recurrence can occur. For example, in the 0.01 a.u. peak-height case, the continuum levels reach their final population by the time the pulse peaks (at $t=t_0$). This time gets successively shorter as we increase the field strength. This shortening of the lifetime of the initial state, which causes the pulse to be effectively shorter, also contributes to the power broadening of the continuum lineshapes.

It is also of interest to look separately at the real and imaginary parts of $b_{E,\mathbf{n}}(t)$, shown in Figs. 2(a) and 2(b) for $\Delta_s=0$. We see that at off-resonance center frequencies the real and imaginary parts oscillate with a frequency of $\sim(\omega_{E,1}-\omega_L)$. This result follows Eq. (7) if we neglect the decay of $b_1(t')$ with time.

We conclude that while a slowly varying continuum leads to a truly irreversible process, in the sense that the ground state decays monotonically in time [see Eq. (45)], the continuum states do not evolve monotonically in time: As we move away from the pulse center, the continuum coefficients tend to increasingly overshoot their final values during the first part of the pulse, resulting in their more and more complete depletion during the second part of the pulse. This trend culminates in the completely off-resonance levels, which rise and fall back to zero as the pulse progresses, forming pure transients. The main difference between the response of a slowly varying continuum to weak pulses relative to strong-pulses is that for strong pulses the above processes are completed sooner in the history of the pulse. Basically b_1 may be completely zero a long time before the end of the pulse, after

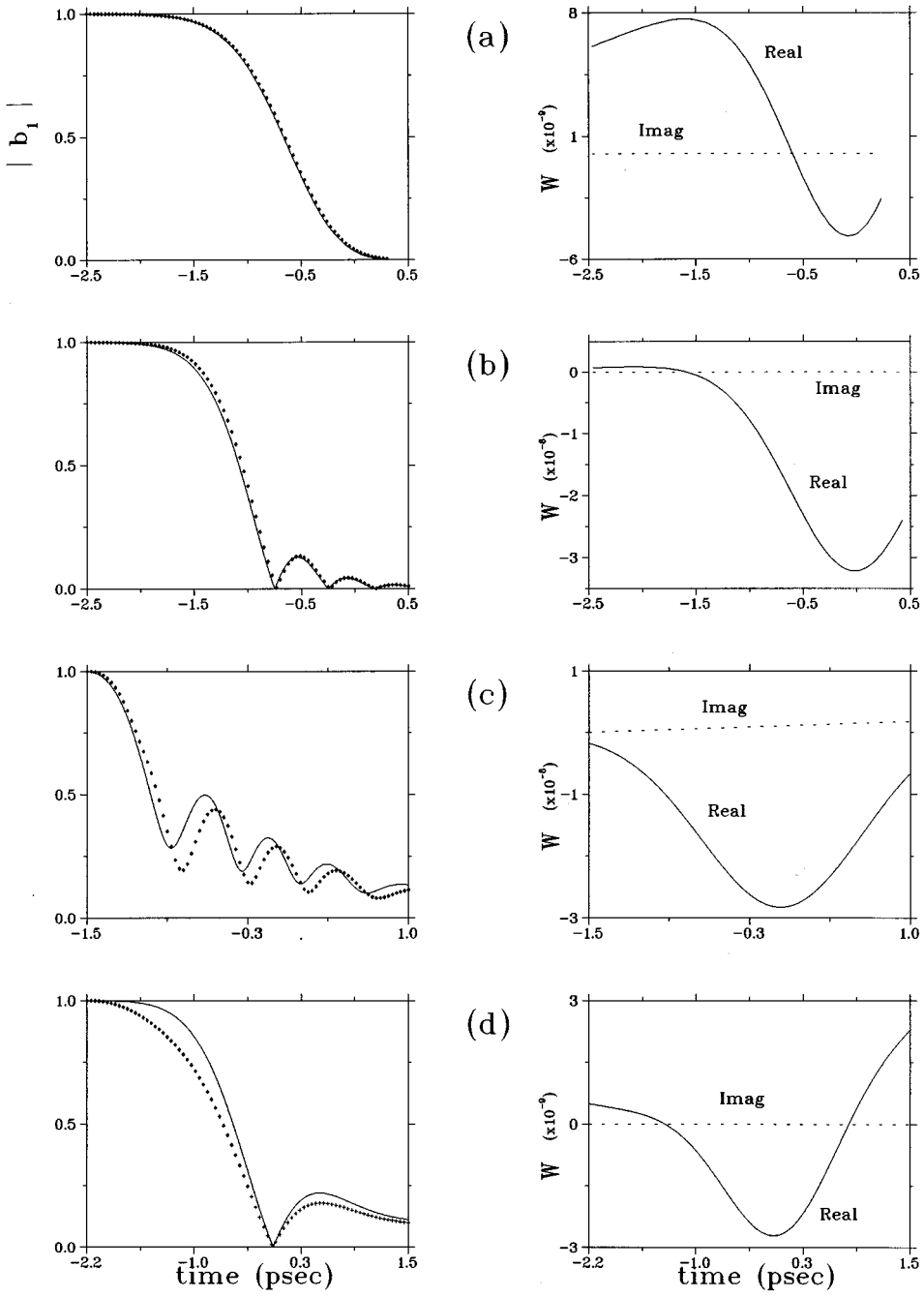

FIG. 8. Time-dependent potential $W(t)$, and $b_1(t)$, the bound-state coefficient. Exact results, full line; uniform approximation, dotted lines. The pulse bandwidth is 20 cm^{-1} and $\mu^2_{s's}=1$. (a) Pulse amplitude $\varepsilon_L=0.005$ a.u., spectral width $\Gamma_s=100$ cm^{-1}, distance from the absorption center $\Delta_s=0$; (b) $\varepsilon_L=0.01$ a.u. $\Gamma_s=50$ cm^{-1}, $\Delta_s=0$; (c) $\varepsilon_L=0.01$ a.u., $\Gamma_s=20$ cm^{-1}, $\Delta_s=10$ cm^{-1}; (d) $\varepsilon_L=0.005$ a.u., $\Gamma_s=20$ cm^{-1}, $\Delta_s=0$.

which point, as follows from Eq. (7), no further dynamics is possible.

The situation is quite different for a *structured* continuum. Figure 3, where the strong-pulse-induced transition to a narrow continuum ($\Gamma_s=50$ cm^{-1}), is displayed, exhibits an intermediate behavior between a ''flat'' continuum and a discrete set of levels. We see that ''center line'', $\omega_{E,1}-\omega_L\approx 0$, levels display recurrences, or Rabi oscillations, similar, though not identical, to those of discrete two-level systems. In contrast, levels at the pulse wings rise and fall smoothly with the pulse, as in the slowly varying continuum case.

The ground-state (b_1) coefficient undergoes oscillations as population is being shunted between the ground state and the continuum states. The b_1 coefficient is plotted together with the center-line $b_{E,\mathbf{n}}$ coefficients in Fig. 4. We see that both the center-line continuum levels and the ground state do not complete even a single Rabi cycle during the pulse duration. In common with discrete two-level systems, the oscillation in each center line $b_{E,\mathbf{n}}$ is in $\pi/2$ phase lag with respect to the oscillation in b_1.

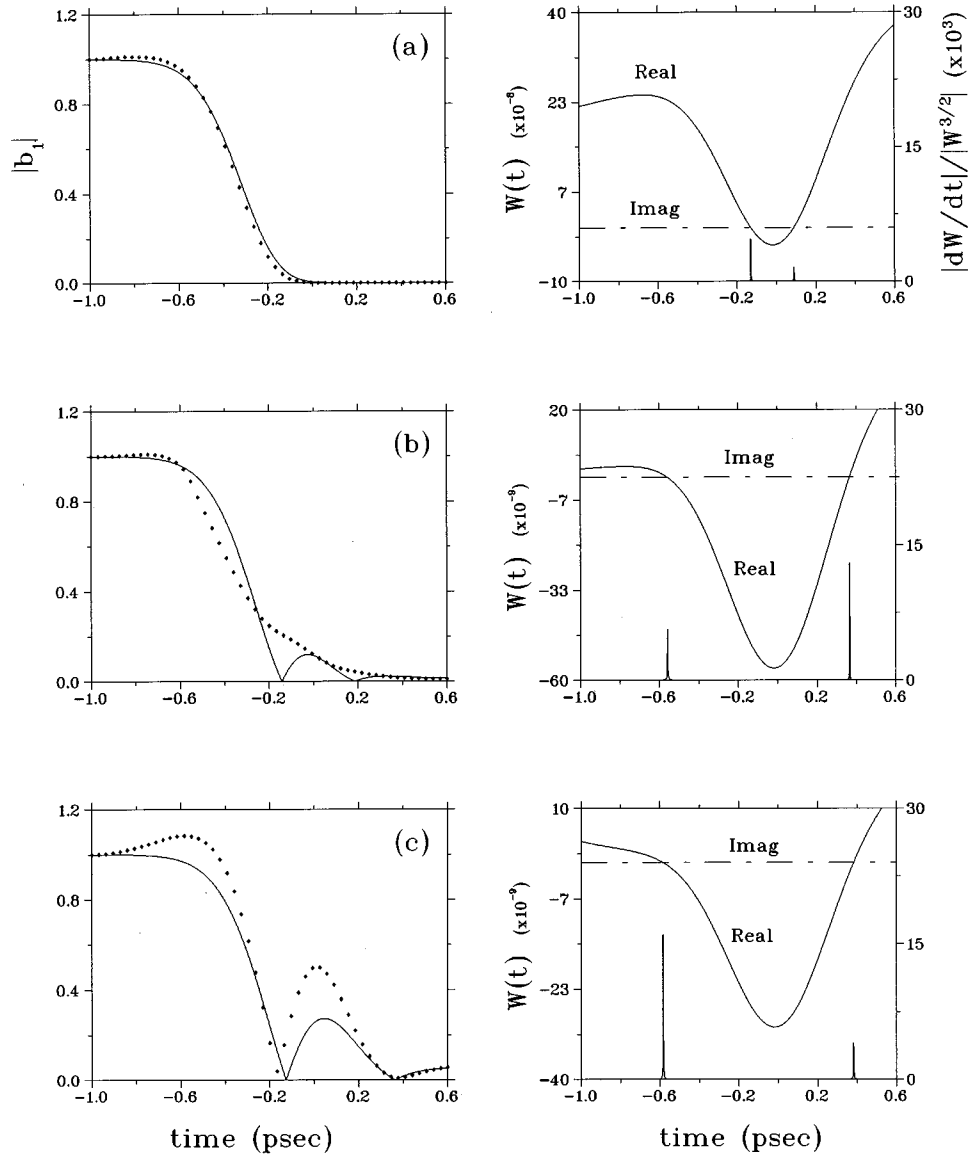

FIG. 9. Left-hand side: The exact b_1 coefficient (full line) and the zero-order WKB approximation (dotted lines). Right-hand side: the ''time-dependent potential'' $W(t)$ and $|W'(t)/[W(t)]^{3/2}|$ when the laser is tuned to the center of the absorption spectrum. Pulse amplitude $=0.01$ a.u., pulse bandwidth$=50$ cm^{-1}. (a) $\Gamma_s=500$ cm^{-1}, (b) $\Gamma_s=100$ cm^{-1}, (c) $\Gamma_s=50$ cm^{-1}.

We now extend the study of narrow-band continua by looking at a continuum composed of *two* distinct diffuse features. In particular, we concern ourselves with the way a strong pulse may alter the line shapes of neighboring resonances. In Figs. 5(a)–5(c) we study pulse absorption by a sum of two Lorentzians. Because this case is obtained by retaining only the $s=s'$ terms in Eq. (17), the bound-continuum transition-dipole matrix elements, shown in Fig. 5(a) by themselves show no interference. However, as shown in Figs. 5(b) and 5(c) as we switch on the pulse, the two initially separated lines begin to merge. For moderate laser powers [Fig. 5(b)], this merging is a signature of saturation: the levels at the center of the absorption lines cease to rise while the population of levels between the line centers continues to increase. At higher laser intensities [Fig. 5(c)], we see the effect of the Rabi cycling: Levels at the line centers oscillate at a higher frequency than levels at the wings of the lines. It may happen, as shown in Fig. 5(c), that the line-center levels execute a 2π cycle and are empty at the end of the pulse, whereas levels away from the line centers execute only a π cycling and are highly populated. Thus, under the action of the strong laser pulse the lines are reversed: the absorption is strongest between the lines and is effectively zero at the resonance ($\mathcal{E}_s$) positions.

As shown in Figs. 6(a)–6(c), the interference is even more dramatic if we allow the resonances to interfere in the weak-field limit by retaining the $s\neq s'$ terms in Eq. (17). We see that as the field becomes strong, the optically induced interference between the lines causes them to cancel the absorption at the end of the pulse for levels midway between the two line centers. As a result, we see three holes in the continuum populations: Two transparent lines at the center of the resonances due to 2π cycling of these levels, accompanied by a third transparent line residing midway between the resonances, due to destructive interference between the resonances.

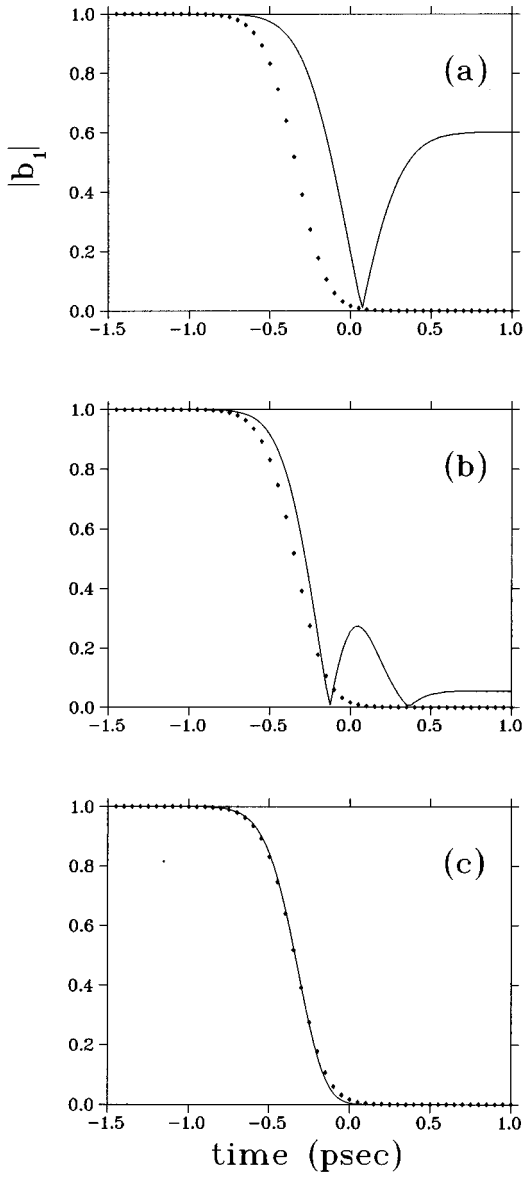

FIG. 10. The SVCA at different spectral widths, for $\mu^2_{s',s}=1$, $\varepsilon_L=0.01$ a.u., pulse bandwidth=50 cm^{-1}, at the center of the absorption spectrum. Exact results are shown in full lines and approximation in dotted lines. (a) $\Gamma_s=10$ cm^{-1}, (b) $\Gamma_s=50$ cm^{-1}, (c) $\Gamma_s=500$ cm^{-1}.

B. The Schrödinger equation, uniform, WKB, and slowly varying continuum approximations

In this subsection we examine how the single Schrödinger equation approximation [Eq. (29)] and other approximations derived from it, in particular the Uniform approximation, compare with the solution of the exact set of equations [Eqs. (20) and (21)]. In addition, we compare the uniform method to the simpler but more approximate zero-order WKB and SVCA methods.

We first study the reduction of the exact set of first-order differential equations [Eqs. (20) and (21)] to the single ''Schrödinger-like'' second-order equation, for an absorption band comprised of several resonances. As shown in Fig. 7, if the field is low to moderately high, so that b_1 does not decay too much, the ''Schrödinger-like'' equation works extremely well. At very high fields, when the ground state begins to undergo Rabi oscillations, the approximation begins to break down.

For a single resonance the ''Schrödinger-like'' equation is exact and we can use it to study further approximations based on it. In Fig. 8(a) we demonstrate the goodness of the uniform approximation at the center of the absorption line (Δ). This is a case in which there is only one effective real-axis turning point. Although the time-dependent potential, $W(t)$, shown in Fig. 8(a) possesses two turning points, one at $t^*\approx-0.5$ psec and one at $t^*\approx0.5$ psec, the $t^*\approx0.5$ psec turning point is not expressed because at that time the b_1 coefficient is essentially 0. Therefore, the problem maps to a single turning point uniform approximation, which, as shown in Fig. 8(a), faithfully reproduces the numerical solution of Eq. (15). As we increase the field intensity, a case shown in Fig. 8(b) the ψ_1 population begins to show an oscillatory behavior. As shown in Fig. 8(b), this is still a single real-axis turning point case and the uniform approximation reproduces perfectly the oscillatory pattern.

In Fig. 8(c) we display a case with relatively small Γ_s and a Δ detuning, for which $W(t)$ possess only complex turning points. In the case shown in Fig. 8(c) the turning point occurs at $t^*=-1.0967-0.1083i$. Here, too, we obtain excellent agreement between the uniform approximation and the exact numerical solutions.

When a second turning point exists while the laser is still on, we need to construct the uniform Airy solutions around each turning point and match the two solutions at some intermediate point. Such a case is shown in Fig. 8(d). Comparison with the exact solution demonstrates that the uniform approximation, while not perfect, works quite well even in this case.

The uniform approximation is more complicated than the primitive WKB method. In most situations it is the only approximation that can be used because it correctly generates solutions across the problematic turning point region(s). In contrast, the zero-order WKB solutions of Eq. (40) do not conserve flux and the first-order WKB solutions diverge at the turning points [due to the $W(t)^{-1/4}$ term]. To show the need for the uniform approximation, a series of computations based on the zero-order WKB approximation for different absorption band widths is displayed in Fig. 9 and compared to the exact results. We see that the zero-order WKB method yields inferior results as compared with the uniform approximation, although at times the zero-order WKB is a reasonable approximation. It has an additional flaw in that it critically depends on the choice of the initial integration time.

The residual term in the zero-order WKB equation, given as $2|dW/dt|/|W^{3/2}|$, can be shown to be roughly proportional to Γ_s^{-2}. Hence, the error in the zero-order WKB approximation is expected to increase with decreasing Γ_s. Thus, choosing a set of pulse intensities such that the zero-order WKB method works well for $\Gamma_s>500$ cm^{-1}, we see that the quality of the approximation deteriorates as Γ_s dips below that value, culminating in the complete breakdown of the approximation when $\Gamma_s\leqslant200$ cm^{-1}. In contrast, the uniform approximation remains valid for values of Γ_s well below 200 cm^{-1}.

A different limit of the uniform approximation leads to the SVCA. In Figs. 10(a)–10(c) examine the effect of the spectral width, at the center of the absorption spectrum (Δ

$=0$). The SVCA, which follows the exact solution faithfully for large values of Γ_s, begins to fail as Γ_s is decreased.

V. CONCLUSIONS

In this paper we have recast the problem of one net photon absorption to a continuum from a strong laser pulse as a single integral equation. We have shown that for a certain class of absorption spectra, this integral equation can be converted to a second-order Schrödinger-like differential equation, which can be accurately solved in an essentially closed form using the semiclassical uniform approximation. Using this methodology we have shown that a transition to continuum is not irreversible if the continuum possesses features narrower than the effective width (reflecting the pulse strength and width) of the pulse. A smooth transition of a given continuum from a perfectly absorbing entity to a set of levels, each executing Rabi oscillations with a precursor bound state, was shown to occur as we increase the pulse strength. As a result of such oscillations, spectral migrations and formations of transparent lines, are shown to occur. The field-induced interferences between neighboring lines has also been also investigated.

In the present work, the basis set of material states has been used. The advantage of this basis set is that it tells us, at every given instant, what is the energetic (kinetic and otherwise) distribution of the material system under the action of the laser field. It also tells us what the material wave packet is doing at any instant of time, a quantity that is also the essence of many purely numerical studies published so far, since all material wave-packet motion is contained in the distribution of the $b_{E,\mathbf{n}}$ coefficients and the properties of the material basis states. Knowledge of the motion of the material wave packet allows us to predict transient quantities associated with spontaneous emission, such as fluorescence and Raman scattering [30,35].

This work clearly demonstrates that the reversibility or irreversibility of a process is a clear function of the mode of preparation of the process. A continuum which appears perfectly flat to a nsec pulse, giving rise to a monotonic decay of the ground state, may appear ''bumpy'' to a fsec pulse, causing as a result transitions from the continuum levels back to the ground precursor state. These conclusions have implications to other sources of irreversibility in nature.

ACKNOWLEDGMENT

The Israel Science Foundation of the Israel Academy is thanked for supporting this paper.

[1] M. Shapiro and R. D. Levine, Chem. Phys. Lett. **5**, 499 (1970); M. Shapiro, J. Chem. Phys. **56**, 2582 (1972).
[2] M. Shapiro, Isr. J. Chem. **11**, 691 (1973).
[3] O. Atabek, J. A. Beswick, R. Lefebvre, S. Mukamel, and J. Jortner, J. Chem. Phys. **65**, 4035 (1976); O. Atabek and R. Lefebvre, Chem. Phys. **23**, 51 (1977); **55**, 395 (1981).
[4] M. D. Morse, K. F. Freed, and Y. B. Band, J. Chem. Phys. **70**, 3620 (1979); Y. B. Band, K. F. Freed, and D. J. Kouri, *ibid.* **74**, 4380 (1981).
[5] K. C. Kulander and J. C. Light, J. Chem. Phys. **73**, 4337 (1980).
[6] G. G. Balint-Kurti and M. Shapiro, Chem. Phys. **61**, 137 (1981); Adv. Chem. Phys. **60**, 403 (1985).
[7] M. Shapiro and R. Bersohn, Ann. Rev. Phys. Chem. **33**, 409 (1982).
[8] E. Segev and M. Shapiro, J. Chem. Phys. **73**, 2001 (1980); **77**, 5601 (1982).
[9] V. Engel, R. Schinke, and V. Stämmler, Chem. Phys. Lett. **130**, 413 (1986); P. Andresen and R. Schinke, in *Molecular Photodissociation Dynamics*, edited by M. N. R. Ashfold and J. E. Baggott (The Royal Society of Chemistry, London, 1987), p. 61; R. Schinke, *Photodissociation Dynamics* (Cambridge University, Cambridge, 1992).
[10] M. Shapiro and H. Bony, J. Chem. Phys. **83**, 1588 (1985).
[11] T. Seideman and M. Shapiro, J. Chem. Phys. **88**, 5525 (1988); **92**, 2328 (1990).
[12] A. D. Bandrauk and O. Atabek, Adv. Chem. Phys. **73**, 823 (1989); S. Chelkowski and A. D. Bandrauk, Chem. Phys. Lett. **186**, 284 (1991); A. D. Bandrauk, J. M. Gauthier, and J. F. McCann, *ibid.* **200**, 399 (1992).
[13] S.-I. Chu, Chem. Phys. Lett. **70**, 205 (1980); T. Ho, C. Laughlin, and S.-I. Chu, Phys. Rev. A **32**, 122 (1985); S.-I. Chu and R. Yin, J. Opt. Soc. Am. B **4**, 720 (1987).
[14] S. O. Williams and D. G. Imre, J. Phys. Chem. **92**, 6636 (1988); J. Zhang and D. G. Imre, Chem. Phys. Lett. **149**, 233 (1988).
[15] V. Engel and H. Metiu, J. Chem. Phys. **92**, 2317 (1990); V. Engel, H. Metiu, R. Almeida, R. A. Marcus, and A. H. Zewail, Chem. Phys. Lett. **152**, 1 (1988); S. Shi and H. Rabitz, J. Chem. Phys. **92**, 364 (1990).
[16] W. Jakubetz, B. Just, J. Manz, and H.-J. Schreier, J. Phys. Chem. **94**, 2294 (1990).
[17] S. Shi and H. Rabitz, J. Chem. Phys. **92**, 364 (1990).
[18] A. D. Hammerich, R. Kosloff, and M. A. Ratner, J. Chem. Phys. **97**, 6410 (1992); A. D. Hammerich, U. Manthe, R. Kosloff, H.-D. Meyer, and L. S. Cederbaum, *ibid.* **101**, 5623 (1994).
[19] E. Charron, A. Guisti-Suzor, and F. H. Mies, Phys. Rev. Lett. **71**, 692 (1993).
[20] A. Bartana, U. Banin, S. Ruhman, and R. Kosloff, Chem. Phys. Lett. **219**, 211 (1994).
[21] M. Crance and M. Aymar, J. Phys. B **13**, L421 (1980).
[22] Z. Deng and J. H. Eberly, Phys. Rev. Lett. **53**, 1810 (1984).
[23] R. Grobe and J. H. Eberly, Phys. Rev. Lett. **68**, 2905 (1992); Phys. Rev. A **48**, 623 (1993); Laser Phys. **3**, 323 (1993); Phys. Rev. A **48**, 4664 (1993).
[24] K. Rzazewski and R. Grobe, Phys. Rev. A **33**, 1855 (1986).
[25] M. Dorr and R. Shakeshaft, Phys. Rev. A **38**, 543 (1988).
[26] K. C. Kulander, Phys. Rev. A **35**, 445 (1987); K. J. Schafer and K. C. Kulander, *ibid.* **42**, 5794 (1990).
[27] R. Blank and M. Shapiro, Phys. Rev. A **50**, 3234 (1994); **51**, 4762 (1995).
[28] P. Brumer and M. Shapiro, Adv. Chem. Phys. **60**, 371 (1985).

[29] B. Piraux, R. Bhatt, and P. L. Knight, Phys. Rev. A **41**, 6296 (1990).
[30] M. Shapiro, J. Chem. Phys. **101**, 3849 (1994).
[31] A. G. Abrashkevich and M. Shapiro, J. Phys. B **29**, 627 (1996).
[32] W. H. Miller, *Modern Theoretical Chemistry, Part B* (Plenum, New York, 1976), Vol. 1.
[33] M. S. Child, *Semiclassical Mechanics with Molecular Applications* (Clarendon Press, Oxford, 1991), pp. 108–112.
[34] C. Cohen-Tannoudji, Bernard Diu, and Franck Laloë, *Quantum Mechanics* (Wiley, New York, 1977), Vol. 2, Chap. XIII.
[35] M. Shapiro, J. Phys. Chem. **97**, 7396 (1993); **99**, 2453 (1993).
[36] E. J. Heller, in *Potential Energy Surfaces; Dynamics Calculations*, edited by D. Truhlar (Plenum, New York, 1981); Acc. Chem. Res. **14**, 368 (1981).
[37] D. E. Amos, Sandia National Laboratories, Netlib/Computer routine library-slatec/Complex Airy and subsidiary routines.
[38] H. Okabe, *Photochemistry of Small Molecules* (Wiley, New York, 1978).